THE ARCHIVE OF MECHANICAL ENGINEERING

VOL. LIX 2012 Number 3

10.2478/v10180-012-0014-1

Key words: Flexible multibody dynamics, beams, circular cross section, absolute nodal coordinate formulation

GRZEGORZ ORZECHOWSKI *

ANALYSIS OF BEAM ELEMENTS OF CIRCULAR CROSS SECTION USING THE ABSOLUTE NODAL COORDINATE FORMULATION

The beam elements, which are widely used in the absolute nodal coordinate formulation (ANCF) can be treated as isoparametric elements, and by analogy to the classical finite element analysis (FEA) are integrated with standard, spatial Gauss-Legendre quadratures. For this reason, the shape of the ANCF beam cross section is restricted only to the shape of rectangle.

In this paper, a distinct method of integration of ANCF elements based on continuum mechanics approach is presented. This method allows for efficient analysis of the ANCF beam elements with circular cross section. The integration of element vectors and matrices is performed by separation of the quadrature into the part that integrate along beam axis and the part that integrate in the beam cross section. Then, an alternative quadrature is used to integrate in the circular shape of the cross section. Since the number of integration points in the alternative quadrature corresponds to the number of points in the standard Gaussian quadrature the change in the shape of the cross section does not affects negatively the element efficiency.

The presented method was verified using selected numerical tests. They show good relatively agreement with the reference results. Apart from the analysis of the beams with the circular cross section, a possibility of further modifications in the methods of the element integration is also discussed. Due to the fact that locking influence on the convergence of the element is also observed, the methods of locking elimination in the proposed elements are also considered in the paper.

1. Introduction

Absolute nodal coordinate formulation (ANCF) [1] is one of the methods for static and dynamic analysis of the flexible multibody systems which undergo large displacements and deformations. This formulation is based on the finite element analysis (FEA) and one of its characteristic is the lack of pure rotational degrees of freedom. Instead of rotations global slopes are used

* *The Institute of Aeronautics and Applied Mechanics, Warsaw University of Technology, ul. Nowowiejska 24, 00-665 Warsaw, Poland; e-mail: gorzech@meil.pw.edu.pl*

in nodes as the nodal coordinates. As a consequence the ANCF elements usually have more coordinates than standard FEA elements but single ANCF element can model more complex deformation modes [2].

In the ANCF, all parameters and shape functions are described with respect to the global, inertial reference frame. The global shape functions must have a complete set of rigid body modes that can describe an arbitrary rigid body translational and rotational displacements. Therefore, element displacement field represents both rigid and flexible body motion. Furthermore the ANCF leads to exact modeling of the rigid body inertia and does not lead to the linearization of the equations of motion as in the case of incremental formulations [3]. ANCF elements are characterized by constant mass matrix and constant gravity force vector and the inertial and centrifugal forces are equal to zero. However, elastic forces are highly nonlinear functions of the body parameters, even in the case of the planar analysis [4].

Moreover, in the ANCF formulation beam and plate elements can be treated as isoparametric elements, which usually do not occur in the case of the classic FEA elements. There are two methods which can be used to formulate the elastic forces in the absolute nodal coordinate formulation. The first method consists in the use of a standard continuum mechanics approach, while in the second method the technical beam theory is used [5].

In the literature many ANCF elements have been proposed. Among them one can found various types of the beam elements, both two-dimensional [6] and three-dimensional [2], as well as different types of the plate elements [7, 8]. Among beam elements in some of the formulations beam kinematics description is used to develop elastic forces [9]. In such a case a shape of the beam cross section can be freely chosen, since appropriate seconds moments of the cross section area appears in the equations. However, the use of the elements that are based on beam kinematics leads to inconsistent definition of the stiffness and mass matrix. Furthermore ANCF beams that are based on the continuum approach allow for capturing the coupled deformation modes including Poisson modes that cannot be captured using existing beam formulations [10]. However, in the absolute nodal coordinate formulation, beams are treated as volumes, so their cross section is usually rectangular. On the other hand, in engineering practice is often necessary to analyze beams with various cross sections. This paper presents the results of a case study when spatial beam element with circular cross section is used. Circular shape of the cross section is chosen because it often occurs in practice. It is also possible to extend this method to the use for other cross section shapes.

This paper is organized as follows. Section 2 shows the spatial beam element used in the paper. Basic kinematic relations of the ANCF formulation are shown as well as the equations of motion in independent coordinates. Sec-

tion 3 presents the consideration associated with integration of the elements with the arbitrary cross section. In addition the method of the integration for circular cross section is shown in detail. Details of the implementation of the presented algorithms are presented in section 4. Section 5 presents several numerical tests, which are used for verification of the presented method. The last section contains short summary of the paper.

2. Equations of motion of the ANCF beam element

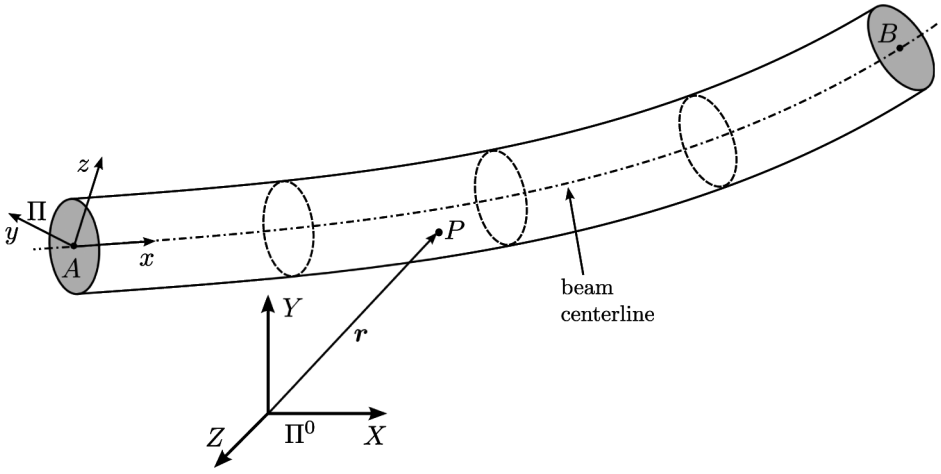

Fig. 1. ANCF beam element

In Fig. 1 the three-dimensional ANCF beam element with two nodes A and B is depicted. The position of the arbitrary point P of the element is described in the global reference frame Π^0. The origin of the local frame Π is placed in beam node A and coordinate x is located along beam axis, while coordinates y and z are perpendicular to the x coordinate.

The presented beam element is fully parametrized [2], so the vector of nodal coordinates contains all three slopes vectors:

$$\boldsymbol{e}_i = \left[\begin{array}{cccc} \boldsymbol{r}_i^T & \left(\dfrac{\partial \boldsymbol{r}_i}{\partial x}\right)^T & \left(\dfrac{\partial \boldsymbol{r}_i}{\partial y}\right)^T & \left(\dfrac{\partial \boldsymbol{r}_i}{\partial z}\right)^T \end{array} \right]^T \tag{1}$$

where vector $\boldsymbol{e}_i$ contains nodal parameters of the i node, vector $\boldsymbol{r}_i$ is the global position vector of the i node, while vectors $\partial \boldsymbol{r}_i/\partial k$ for $k = x, y, z$ are gradients of the position vector (slopes) in the i node. Then vector of the nodal coordinates for single element may be given as follows:

$$\boldsymbol{e} = \left[\begin{array}{cc} \boldsymbol{e}_A^T & \boldsymbol{e}_B^T \end{array} \right]^T \tag{2}$$

Using the vector of nodal coordinates from Eq. 2, one can get the position of the arbitrary point on the element:

$$\boldsymbol{r} = \boldsymbol{S}\boldsymbol{e} \tag{3}$$

where $\boldsymbol{S} = \boldsymbol{S}(x, y, z)$ is the matrix that contains element shape functions. Matrix $\boldsymbol{S}$ depends only on the spatial coordinates and it may be given in the form [2]:

$$\boldsymbol{S} = [s_1\boldsymbol{I}\ s_2\boldsymbol{I}\ s_3\boldsymbol{I}\ s_4\boldsymbol{I}\ s_5\boldsymbol{I}\ s_6\boldsymbol{I}\ s_7\boldsymbol{I}\ s_8\boldsymbol{I}] \tag{4}$$

where $\boldsymbol{I}$ is the identity matrix of size 3×3, whereas functions s_i for $i = 1, \ldots, 8$ are given by:

$$\begin{cases} s_1 = 1 - 3\xi^2 + 2\xi^3, & s_2 = l(\xi - 2\xi^2 + \xi^3), \\ s_3 = l(\eta - \xi\eta), & s_4 = l(\zeta - \xi\zeta), \\ s_5 = 3\xi^2 - 2\xi^3, & s_6 = l(-\xi^2 + \xi^3), \\ s_7 = l\xi\eta, & s_8 = l\xi\zeta \end{cases} \tag{5}$$

where l is the length of the element in the undeformed state, while ξ, η and ζ are the element natural coordinates, given by:

$$\xi = \frac{x}{l} \quad \eta = \frac{y}{l} \quad \zeta = \frac{z}{l} \tag{6}$$

The kinetic energy of the single element may be written by the following formula:

$$T = \frac{1}{2}\int_V \rho \dot{\boldsymbol{r}}^T \dot{\boldsymbol{r}} dV = \frac{1}{2}\dot{\boldsymbol{e}}^T \boldsymbol{M}\dot{\boldsymbol{e}} \tag{7}$$

where ρ and V are, respectively, density and volume of the element while $\boldsymbol{M}$ is mass matrix of the element. After differentiation of Eq. 3 with respect to time, mass matrix can be written as follows:

$$\boldsymbol{M} = \int_V \rho \boldsymbol{S}^T \boldsymbol{S} dV \tag{8}$$

The mass matrix of ANCF beam element is constant.

In the absolute nodal coordinate formulation, Coriolis, tangential, centrifugal as well as other forces resulting from differentiation of the kinetic energy are equal to zero. Thus, the nonzero terms in system equations of motion come from the vectors of the elastic and external forces. The elastic forces are given by:

$$\boldsymbol{Q}_s = \left(\frac{\partial U_s}{\partial \boldsymbol{e}}\right)^T \tag{9}$$

where U_s is the energy of the elastic deformation. Elastic energy is written as a function of the Green-Lagrange strain vector $\boldsymbol{\varepsilon}$ and second Piola-Kirchhoff stress vector $\boldsymbol{\sigma}$, as follows:

$$U_s = \frac{1}{2}\int_V \boldsymbol{\varepsilon}^T \boldsymbol{\sigma} dV \tag{10}$$

While, for the model of linear-elastic material, we have the following relation between strain and stress vectors:

$$\boldsymbol{\sigma} = \boldsymbol{E}\boldsymbol{\varepsilon} \tag{11}$$

where $\boldsymbol{E}$ is a matrix of the material constants.

Therefore, to calculate the vector of elastic forces it is necessary to calculate only the strain vector:

$$\boldsymbol{\varepsilon}_m = \frac{1}{2}(\boldsymbol{J}^T\boldsymbol{J} - \boldsymbol{I}) \tag{12}$$

where $\boldsymbol{\varepsilon}_m$ is symmetric Green-Lagrange strain tensor associated with the strain vector $\boldsymbol{\varepsilon}$ and $\boldsymbol{J}$ is a matrix of deformation gradient:

$$\boldsymbol{J} = \frac{\partial \boldsymbol{r}}{\partial \boldsymbol{X}} \tag{13}$$

Eqs. 10 and 11 can be substituted into Eq. 9 to obtain:

$$\boldsymbol{Q}_s = \int_V \left(\frac{\partial \boldsymbol{\varepsilon}}{\partial \boldsymbol{e}}\right)^T \boldsymbol{E}\boldsymbol{\varepsilon} dV \tag{14}$$

Vector of the external forces, which include the gravitational forces, can be derived using the principle of virtual work as follows:

$$\delta W_e = \boldsymbol{Q}_e{}^T \delta \boldsymbol{e} \tag{15}$$

where δW_e is the virtual work of the external forces and $\boldsymbol{Q}_e$ is the vector of the generalized external forces.

Finally, one can write the equations of motion in the independent coordinates for the three-dimensional ANCF beam as follows [11]:

$$\boldsymbol{M}\ddot{\boldsymbol{e}} + \boldsymbol{Q}_s = \boldsymbol{Q}_e \tag{16}$$

3. Integration of the element matrices for beam element with circular cross section

Equations of motion for ANCF beam element were derived without any assumption about the shape of the beam i.e. they are valid theoretically for the arbitrarily shaped beam elements. However due to the limited degree of the approximating polynomials the full freedom of the element shape choice is not desirable. For the beam elements, it is especially important to have a leading dimension (length) but shape of the cross section may be changed.

In the case of the classic FEA beam elements integration of the matrices for the equations of motion is performed only along the beam axis. The inertia of the cross section is taken into account with the use of the appropriate moments of area. In the ANCF the shape of the element is taken into account through appropriate integration of the integrals of Eqs. 8 and 14. ANCF beams can be integrated like the volumetric FEA elements by means of a spatial Gauss-Legendre quadrature [5]. In the classical FEA quadratures for tetrahedral and solid (prism) shapes are used. For the beam elements, only the quadrature for solid shape may be used and therefore the shape of the cross section of ANCF elements in undeformed state is limited only to the shape of rectangle. Consequently, in order to allow for other cross section shapes, it is necessary to introduce different formulations for the quadrature.

To integrate expressions in three dimensions with Gaussian quadrature, one dimensional integration formulas may be apply successively in each direction [5]:

$$G = \int_V g(\xi,\eta,\zeta)dV = \int_{a_1}^{b_1}\int_{a_2}^{b_2}\int_{a_3}^{b_3} g(\xi,\eta,\zeta)d\xi d\eta d\zeta \approx \sum_{i=1}^{m}\sum_{j=1}^{n}\sum_{k=1}^{o} w_1(i)w_2(j)w_3(k)g[\xi(i),\eta(j),\zeta(k)] \quad (17)$$

where a_h, b_h and w_h for $h = 1,2,3$ are, respectively, lower and upper integration limits and the quadrature weights; $\xi(i)$, $\eta(j)$ and $\zeta(k)$ are quadrature points, while m, n and o are quadrature orders in direction of the ξ, η and ζ axis, respectively. In turn, $g(\xi,\eta,\zeta)$ is the integrand dependent from the element natural coordinates. In general, g may be a vector or matrix function.

If in Eq. 17 g is a polynomial function, the Gaussian quadrature gives the exact result for a polynomial degree up to $2p-1$, where p is the order of the quadrature. In general, in the FEA and ANCF we are dealing with polynomials so quadrature orders are chosen in such a way that integration is accurate.

Using Eq. 17 one can split integration into appropriate parts:

$$G = \int_{a_1}^{b_1} \int_A g(\xi, \eta, \zeta) dA d\xi \approx \sum_{i=1}^{m} w_1(i) \int_A g[\xi(i), \eta, \zeta] dA, \quad dA = d\eta d\zeta \tag{18}$$

where A is the cross section area. In the case when standard Gaussian quadrature is applied, the cross section is rectangular. However, one can apply integration schema for another cross sectional shape. For the circular shape of the cross section, the following quadrature may be applied [12]:

$$\int_A h(\eta, \zeta) dA \approx \frac{\pi}{s} \sum_{j=1}^{s} \sum_{k=1}^{s} w(k) h[\eta(j,k), \zeta(j,k)], \quad A = \{(\eta, \zeta) : \eta^2 + \zeta^2 \leq 1\} \tag{19}$$

where $h(\eta, \zeta) = g[\xi(i), \eta, \zeta]$ for a fixed ξ, while s is the order of the quadrature. The presented quadrature for the circle uses s^2 for even s and $s^2 - s + 1$ for odd s integration points. If function h, which appear in Eq. 19 is a polynomial, then using the presented quadrature one can accurately integrate it up to the degree of $2s - 1$.

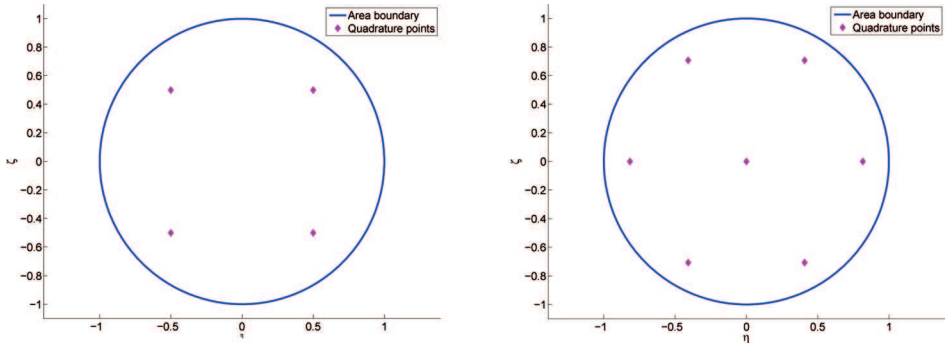

Fig. 2. Quadrature points for $s = 2$ and $s = 3$

Fig. 2 presents quadrature integration points from Eq. 19 for the unit circle and quadrature orders equals to 2 and 3.

In Tab. 1 the values of weights w and parameters r, t and q are shown. Using the values of the r, t and q, one can evaluate quadrature points from Eq. 19 as:

$$\eta(j,k) = q(j)r(k), \quad \zeta(j,k) = t(j)r(k) \tag{20}$$

4. Implementation

The method for modeling beams with circular cross section was applied to the spatial beam [2] shown in Fig. 1. Elastic force for this element can

Table 1.

Quadrature points

Order	r	t	q	w
1	0	0	1	1
2	$\pm\frac{\sqrt{2}}{2}$	$\pm\frac{\sqrt{2}}{2}$	$\frac{\sqrt{2}}{2}$	$\frac{1}{2}$
3	0	0	1	$\frac{1}{4}$
	$\pm\frac{\sqrt{6}}{3}$	$\pm\frac{\sqrt{3}}{2}$	$\frac{1}{2}$	$\frac{3}{8}$
4	$\pm\sqrt{\frac{3+\sqrt{3}}{6}}$	$\pm\sqrt{\frac{2+\sqrt{2}}{4}}$	$\sqrt{\frac{2-\sqrt{2}}{4}}$	$\frac{1}{4}$
	$\pm\sqrt{\frac{3-\sqrt{3}}{6}}$	$\pm\sqrt{\frac{2-\sqrt{2}}{4}}$	$\sqrt{\frac{2+\sqrt{2}}{4}}$	$\frac{1}{4}$

be calculated using Eq. 14. In the computation of the elastic forces the exact integration is performed with 5, 3 and 3 quadrature points in ξ, η and ζ directions, respectively. However, one can speeds up the computations without apparent loss of accuracy if the number of integration points is reduced by one, to 4, 2 and 2 in ξ, η and ζ directions, respectively [13]. This gives a four integration points in the cross section.

Similarly, using the quadrature for circular cross section of the Eq. 19 the exact integration is performed with third order quadrature which gives seven integration points in section. Numerical tests show, however, that without apparent loss of accuracy the order of the quadrature can be reduced to two which gives four integration points. Therefore, regardless of the kind of beam being analyzed, with rectangular or circular cross sections, the same number of quadrature points is used. Eq. 19 presents quadrature for circular section with unit radius. In order to integrate equations with arbitrary radius R, one may use the following relationship:

$$\int_A h(\eta,\zeta)dA \approx \frac{\pi\Gamma^2}{s}\sum_{j=1}^{s}\sum_{k=1}^{s} w(k)h[\Gamma\eta(j,k),\Gamma\zeta(j,k)],$$

$$A=\{(\eta,\zeta):\eta^2+\zeta^2\le R\} \quad (21)$$

where $\Gamma = R/l$.

The relationships derived above were implemented in the computer program written in the MATLAB language [14]. In order to integrate the equa-

tions of motion, the Newmark procedure was used [5]. Two versions of the Newmark procedure were implemented – in the first one the time step was fixed during integration and in the second one the time step was chosen in an adaptive way with error control [15]. The results of the numerical test were compared with known analytical solutions and with simulation results performed with a commercial FEA package [16].

5. Numerical tests

In order to verify the proposed solution, several static and dynamic numerical tests were performed.

5.1. Static bending

In the first test, we analyzed the displacements of the clamped beam. The beam was loaded at the free end with the constant bending moment. The exact value of the bending moment is known when the beam takes the shape of the perfect circle [17]:

$$M = \frac{2\pi EI}{l} \tag{22}$$

where E is the Young's module of the beam, while I is the second moment of beam area according to the axis parallel to the direction of moment vector.

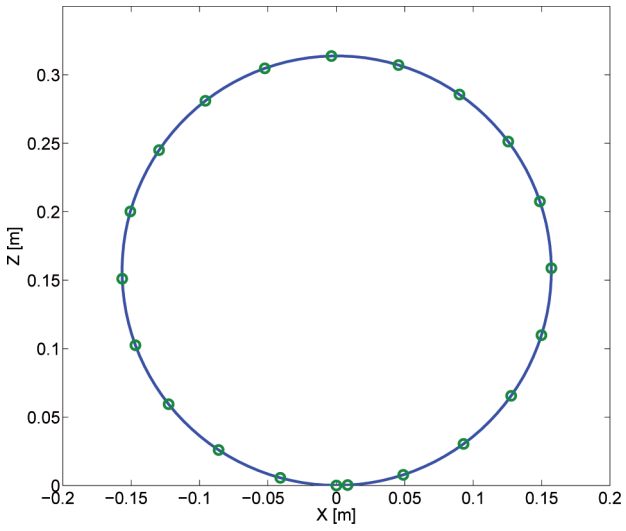

Fig. 3. Static bending of the beam

Fig. 3 shows the results for bending of the beam of 1m length and bending stiffness $EI = 2.513 \times 10^4$ Nm^2 (for $E = 2 \times 10^{11}$ Pa and $R = 0.02$

m). To avoid volumetric locking problems, the Poisson ratio was set to zero [18]. The analysis was performed with twenty ANCF elements. Such a large number of elements was used to avoid problems with other lockings, mainly the shear locking. The results presented in Fig. 3 shows that the beam tooks an almost perfect circular shape. The end point is shifted about a 8.3 mm with respect to the clamped point. Like in the case of the standard beam element with rectangular cross section the correct result is obtained only for moderately thick beams.

5.2. Physical pendulum

The next simulation examined the movement of a physical pendulum in the gravitational field. The pendulum was placed horizontally at the initial position. The pendulum is one meter long with the Young's module $E = 2 \times 10^7$Pa, Poisson ratio $\nu = 0.3$ or 0, density $\rho = 7200$kg/m^3 and with the circular cross section with the radius $R = 0.01$m. In the simulations, six to ten ANCF finite elements were used.

The simulation results performed with ANCF beam elements are compared with the results of simulations carried out in the FEA package [16] using two node beam element BEAM188 which may include any shape of the cross section. In the classical FEA simulation, ten finite elements were used.

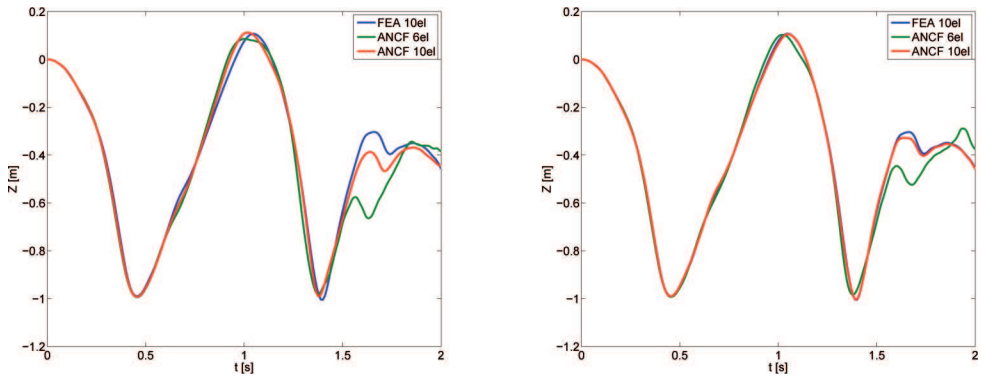

Fig. 4. Displacements of the physical pendulum (for $\nu = 0.3$ and $\nu = 0$)

In Fig. 4 the displacements of the end of the pendulum versus time are presented. All the results show good agreement but during last 0.5s of the simulation the results obtained using ten ANCF elements are in better agreement with FEA then the results obtained with only six elements. Also simulations in which the Poisson ratio is set to zero (right figure) lead to a better agreement with the FEA solution. This happen probably due to the Poisson locking phenomenon. It may be also noticed (Fig. 4) that the rate of

convergence in the case of the third-order ANCF beam element is similar to that of the linear FEA beam element. The slow convergence is the result of the presence of locking, especially shear locking [19].

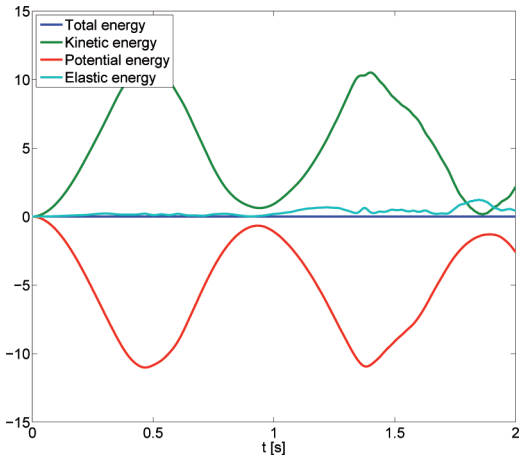

Fig. 5. Total energy of the physical pendulum

Fig. 5 presents the plot of the total energy for the pendulum moving in the gravitational field. As one can see, energy is preserved for whole simulation time.

To solve equations of motion Newmark algorithm with error control and automatized integration time step selection [15] was used. Attempts were made to solve those equations with fixed step Newmark method but the solution did not converge, despite the fact that in similar simulations for a beam with rectangular cross section such problems were not observed. Consideration of this issue may require additional attention.

5.3. Dynamic bending of the clamped beam

The last example presents dynamic bending of the beam clamped on the one end and loaded by variable force on the free end. Like in the previous simulations, the beam has the length $l = 1\text{m}$ and density $\rho = 7200\text{kg/m}^3$. Young's module is increased to $E = 2 \times 10^{11}\text{Pa}$ and the radius is reduced to $R = 2.5\text{mm}$. The force acting on the free end is perpendicular to the beam axis, in the undeformed state, and changes linearly in its magnitude from 0 to 1N during one-second simulation. Results of the tests are compared with the analogous simulations performed in FEA package. As in the previous example, the BEAM188 beam element was used.

Displacements of the beam are shown in Fig. 6. As one can see when the Poisson ratio is set to zero (bottom plot), the simulations using ANCF and

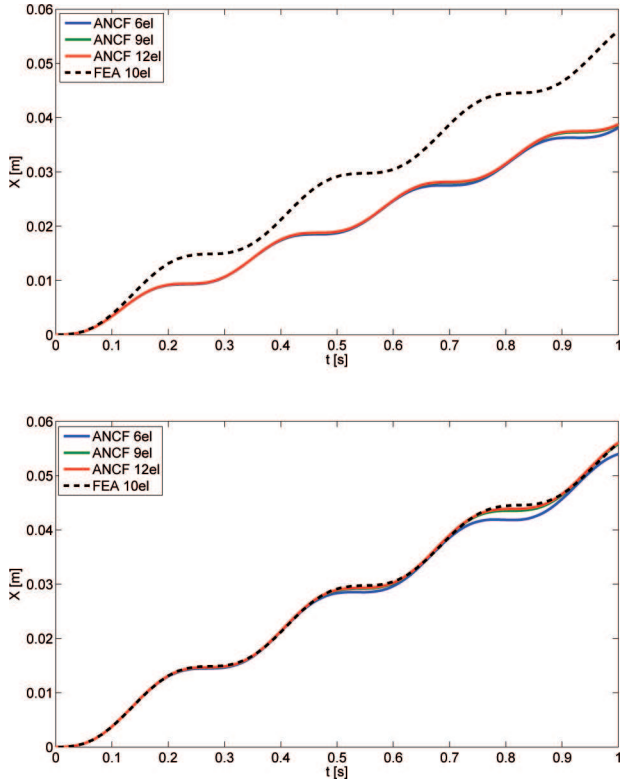

Fig. 6. Displacements of the clamped beam ($\nu = 0.3$ and $\nu = 0$)

FEA formulations are in very good agreement, irrespective of the number of used elements. On the other hand, the upper plot shows huge differences between the results. Even when number of the elements increases for ANCF simulations, one can be notice that the results converge to the wrong solution. It is very likely that these convergence problems are caused by Poisson locking.

6. Conclusions

The paper presents a method for analyzing three dimensional ANCF beam element with circular cross section based on the continuum mechanics approach. The selected method of integration for this shape of the cross section is discussed and the possibility of inclusion of beams with other cross section shapes is also shown. Through further modifications of the integration schema additional properties of the element can be introduced, such as taper cross section, occurring in the BEAM188 element.

For the verification of the results, several numerical test were performed. A good agreement with the reference solutions is observed in cases where

influence of the element locking is small. In other cases, there is a clear difference between ANCF and reference results as presented in the literature [19, 18]. In order to eliminate locking effects, various standard techniques may be applied to the element proposed in this paper, such a higher order elements, selective reduced integration or the assumed strain method [13].

Manuscript received by Editorial Board, May 26, 2012;
final version, June 11, 2012.

REFERENCES

[1] Shabana A.A.: Definition of the Slopes and the Finite Element Absolute Nodal Coordinate Formulation. Multibody System Dynamics, 1997, vol. 1, No 3, pp. 339-348.
[2] Shabana A.A., Yakoub R.Y.: Three Dimensional Absolute Nodal Coordinate Formulation for Beam Elements: Part I and II. Journal of Mechanical Design, 2001, vol. 123, No 4, pp. 606-621.
[3] Shabana A.A.: Finite Element Incremental Approach and Exact Rigid Body Inertia. Journal of Mechanical Design, 1996, vol. 118, No 2, pp. 171-178.
[4] Berzeri M., Shabana A.A.: Development of simple models for the elastic forces in the absolute nodal co-ordinate formulation. Journal of Sound and Vibration, 2000, vol. 235, No 4, pp. 539-565.
[5] Bathe K.J.: Finite Element Procedures. New Jersay, Prentice Hall, 1996.
[6] Omar M.A., Shabana A.A.: A two-dimensional shear deformable beam for large rotation and deformation problems. Journal of Sound and Vibration, 2001, vol. 243, No 3, pp. 565-576.
[7] Dmitrochenko O.N., Pogorelov D.Y.: Generalization of Plate Finite Elements for Absolute Nodal Coordinate Formulation. Multibody System Dynamics, 2003, vol. 10, No 1, pp. 17-43.
[8] Mikkola A.M., Shabana A.A.: A Non-Incremental Finite Element Procedure for the Analysis of Large Deformation of Plates and Shells in Mechanical System Applications. Multibody System Dynamics, 2003, vol. 9, No 3, pp. 283-309.
[9] Yoo W.S., Lee J.H., Park S.J., Sohn J.H., Dmitrochenko O.N., Pogorelov D.Y.: Large Oscillations of a Thin Cantilever Beam: Physical Experiments and Simulation Using the Absolute Nodal Coordinate Formulation. Nonlinear Dynamics, 2003, vol. 34, No 1, pp. 3-29.
[10] Maqueda L.G., Shabana A.A.: Poisson modes and general nonlinear constitutive models in the large displacement analysis of beams. Multibody System Dynamics, 2007, vol. 18, No 3, pp. 375-396.
[11] Shabana A.A.: Computational Continuum Mechanics, Cambridge, Cambridge University Press, 2008.
[12] Ronald C., Kyung J.K.: A survey of known and new cubature for the unit disk. Katholieke Universiteit Leuven, TW 300, 2000.
[13] Gerstmayr J., Shabana A.A.: Efficient integration of the elastic forces and thin three-dimensional beam elements in the absolute nodal coordinate formulation, Multibody Dynamics 2005 ECCOMAS Thematic Conference, 2005 (CDROM).
[14] MATLAB User's Guide, Release R2011b, 2011, The MathWorks, Inc.
[15] Li X.D., Zeng L.F., Wiberg N.-E.: A simple local error estimator and an adaptive time-stepping procedure for direct integration method in dynamic analysis. Communications in Numerical Methods in Engineering, 1993, vol. 9, No 4, pp. 273-292.
[16] ANSYS Mechanical APDL Documentation, Release 13.0, SAS IP, Inc., 2010.

[17] Sugiyama H., Suda Y.: A curved beam element in the analysis of flexible multi-body systems using the absolute nodal coordinates. Proceedings of the Institution of Mechanical Engineers, Part K: Journal of Multi-body Dynamics, 2006, vol. 221, No 2, pp. 219-231.
[18] Schwab A.L., Meijaard J.P.: Comparison of Three-Dimensional Flexible Beam Elements for Dynamic Analysis: Classical Finite Element Formulation and Absolute Nodal Coordinate Formulation. Journal of Computational and Nonlinear Dynamics, 2010, vol. 5, No 1, pp. 011010.
[19] Gerstmayr J., Shabana A.A.: Analysis of Thin Beams and Cables Using the Absolute Nodal Co-ordinate Formulation. Nonlinear Dynamics, 2006, vol. 45, No 1, pp. 109-130.

Analiza elementów belkowych o kołowym kształcie przekroju poprzecznego z zastosowaniem opisu w globalnych współrzędnych węzłowych

Streszczenie

Elementy belkowe, które są często stosowane w sformułowaniu w globalnych współrzędnych węzłowych (GWW), mogą być traktowane jak elementy izoparametryczne, zatem przez analogię do elementów klasycznej metody elementów skończonych (MES) są całkowane z zastosowaniem standardowej, przestrzennej kwadratury Gaussa-Legendre. Z tego powodu, kształt elementów belkowych GWW jest ograniczony do kształtu prostokąta.

W artykule przedstawiono alternatywną metodę całkowania macierzy w elementach GWW, w których siły sprężystości są liczone z zastosowaniem zależności konstytutywnych teorii sprężystości. Opisywana metoda pozwala na wydajną analizę elementów z kołowym przekrojem poprzecznym. Całkowanie wektorów oraz macierzy elementów przeprowadzono poprzez rozdzielenie kwadratury na część całkującą względem osi elementu oraz część całkującą w przekroju poprzecznym elementu. Następnie zastosowano alternatywną kwadraturę do kołowego kształtu przekroju poprzecznego. Liczba punktów całkowania zastosowanej kwadratury jest równa liczbie punktów całkowania standardowej kwadratury Gaussa, przez co zmiana kształtu przekroju poprzecznego nie wpłynęła negatywnie na wydajność elementu. Przedstawiona metoda została zweryfikowana z zastosowaniem wybranych testów numerycznych. Testy pokazały dobrą zgodność z wynikami referencyjnymi. Obok analizy elementów z kołowym przekrojem poprzecznym, przeprowadzono dyskusję dalszych modyfikacji schematu całkowania elementów. Ze względu na zaobserwowanie negatywnego wpływu blokad na zbieżność rozwiązania elementów, w artykule przedstawiono metody ich eliminowania.